

Measurement of the temperature dependence of the rate at which muonic molecules of deuterium are formed for various spin states of the $d\mu$ atoms at high deuterium density

V. P. Dzheleпов, V. G. Zinov, S. A. Ivanovskii, S. B. Karpov, A. D. Konin, A. I. Malyshev, L. Marczis, D. G. Merkulov, A. I. Rudenko, V. V. Fil'chenkov, and O. A. Yurin

Joint Institute for Nuclear Research

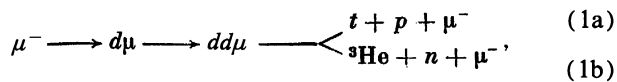
(Submitted 9 July 1991)

Zh. Eksp. Teor. Fiz. **101**, 1105–1117 (April 1992)

The temperature dependence of the rate at which $dd\mu$ molecules form from two hyperfine-structure states of the $d\mu$ atom has been measured in experiments with dense deuterium ($\phi \approx 1$). The rate of transitions between these states has also been measured. The results are compared with the results of measurements by the Vienna-Villengen group, carried out at low deuterium densities ($\phi = 0.02$ and 0.04). The comparison suggests that a density effect may be operating in the production of $dd\mu$ molecules from the state of the $d\mu$ atom with a spin $F = 3/2$. This interpretation agrees with the predictions of the theory of resonant production of muonic molecules which incorporates, along with the Wessmann mechanism, collisional broadening of the resonance.

1. BACKGROUND OF THE STUDY

Experiments on muon catalysis of the fusion of deuterium nuclei,



(1b)

have been a foundation for the physics of the resonance production of muonic molecules. In the course of research on this process, the resonance production of μ molecules was detected experimentally.¹ This production process has since been explained^{2,3} and has more recently been confirmed directly by measurements of the temperature dependence of the rate ($\lambda_{dd\mu}$) of process (1) (Ref. 4). Yet another manifestation of the resonant nature of the process by which $dd\mu$ molecules form is the sharp difference in the rates at which $dd\mu$ molecules are produced from the upper and lower hyperfine states of the $d\mu$ atom. This difference was first observed in an experiment⁵ by the Vienna-Villengen group (a collaboration of the Austrian Academy of Sciences and the P. Scherer Institute, respectively).

Process (1) continues to be the subject of active research. At an international conference on the problem of muon-catalyzed fusion held in Vienna in 1990, for example, three experimental papers reported measurements of the temperature dependence $\lambda_{dd\mu}(T)$. These papers were by a group from the Leningrad Institute of Nuclear Physics, Academy of Sciences of the USSR,⁶ a group from the Joint Institute for Nuclear Research,^{7,8} and the Vienna-Villengen group.⁹ This situation can be explained by the following circumstances.

1. After the first striking successes in research on the muon catalysis of the $d + t$ fusion reaction, it became apparent that there were major difficulties in interpreting the experimental data. The situation is aggravated by the complexity of the kinetics of μ -atomic and μ -molecular effects in a mixture of D_2 and T_2 . The process (1) is far more attractive from this standpoint, because here the basic ideas of the theory can be tested in a fairly simple and convincing way.

2. The theory of muon-catalyzed fusion by reaction (1) has recently made significant advances. This progress includes calculations of the matrix elements for the rate of process (1) (Refs. 10–13) and an accurate (0.1-meV!) calculation of the energies of the resonant transitions. In the latter case, it is of fundamental importance to carry out precise calculations of the Coulomb energy of the weakly bound level with $J = \nu = 1$ in the $dd\mu$ molecule and also to accurately incorporate relativistic corrections to this energy. Among these corrections, it turns out that the contribution from the vacuum polarization dominates.^{14–16} It follows from the theory that measurements of the temperature dependence of the rate of production of $dd\mu$ molecules separately for each hyperfine state of the $d\mu$ atom, with spins $F = 3/2$ and $F = 1/2$ ($\lambda_{3/2}$ and $\lambda_{1/2}$), would make it possible to carry out a comprehensive test of the theory, including a precise determination of the energy $\varepsilon_{1,1}$ of the weakly bound level with $J = \nu = 1$ in a system of $dd\mu$ molecules.^{14–16}

3. Finally, we should mention the possibility of studying the so-called collisional broadening of the resonance¹⁷ in the production of $dd\mu$ molecules. This effect, which dominates in the production of $d\mu$ molecules, should be seen (according to the theoretical predictions) in the process (1) only in measurements of the quantity $\lambda_{3/2}$, and then only at a high deuterium density, $\phi \approx 1$ (Refs. 11–13). (As usual, the density is expressed in relative units: $\phi = n/n_0$, where $n_0 = 4.25 \cdot 10^{22}$ nuclei/cm³ is the density of liquid hydrogen.) It follows that a correct evaluation of the contribution from collisional broadening of the resonance requires a comparison of measurements of the temperature dependence $\lambda_{3/2}(T)$ at low and high deuterium densities.

Figure 1 shows the conditions of the previous experiments^{6–9,18–20} on the process (1). In characterizing these measurements, we should point out two circumstances.

1) The measurements made by the other groups were carried out with deuterium of low density, $\phi \ll 0.1$.

2) Only in the experiments of Refs. 9 and 18 was the $\lambda_{dd\mu}(T)$ dependence found separately for each hyperfine

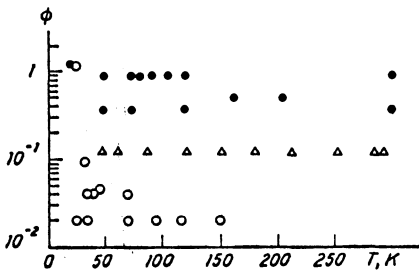


FIG. 1. Parameter values of the experiments of Refs. 6–9 and 18–20 and of the present measurements. The deuterium density is expressed in units of $\phi = n/n_0$, where $n_0 = 4.25 \cdot 10^{22}$ nuclei/cm³ is the density of liquid hydrogen. ●—The present study and previous measurements by our group,^{7,8,20} ○—experiments of Refs. 9 and 18; △—experiments of Refs. 6 and 19.

state of the $d\mu$ atom. In our studies^{7,20} and in experiments by the group from the Leningrad Institute of Nuclear Physics,^{6,19} what was determined was the rate at which $dd\mu$ molecules are produced, averaged over the spin states (the steady-state rate), as a function of the temperature. (Estimates of $\lambda_{3/2}$ were found in Ref. 8.)

Our goal in the present study was to measure the temperature dependence $\lambda_{3/2}(T)$ and $\lambda_{1/2}(T)$ at high deuterium density, $\phi \approx 1$. We were particularly interested in the temperature interval $T = 80$ – 120 K, in which we would expect the density effect to be most obvious, because of the collisional broadening of the resonance. The experimental method involves detecting neutrons from the muon catalysis of reaction (1b) with the help of a gaseous deuterium target. This method was originally proposed in Ref. 4 to study muon catalysis. Since then, it has been adopted widely in various laboratories.

2. KINETICS OF MUON CATALYSIS IN DEUTERIUM

Figure 2 is a schematic diagram of the primary μ -atomic and μ -molecular processes in deuterium. The $d\mu$ atoms are produced in two hyperfine states, with spins $F = 3/2$ and $F = 1/2$, with respective probabilities of $2/3$ and $1/3$. These atoms then undergo thermalization. According to calculations of the cross section for the scattering of $d\mu$ atoms in deuterium,²¹ the time scale for the slowing from an initial energy $E_0 = 1/2$ eV to $E = 0.003$ eV is $1/\phi$ ns. Spin-exchange transitions of the type $(F = 3/2) - (F = 1/2)$ can occur in collisions of $d\mu$ atoms with deuterons. At tempera-

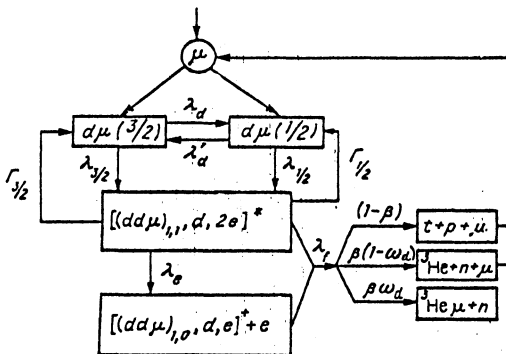


FIG. 2. Schematic diagram of muon catalysis in pure deuterium.

tures $T \leq 120$ K, these transitions are irreversible, since the energy of the hyperfine splitting is $\Delta E_{\text{hf}} = 0.048$ eV.

The production of muonic molecules $dd\mu$ occurs from these spin states of the $d\mu$ atom at rates $\lambda_{3/2}$ and $\lambda_{1/2}$, respectively. The rate of the usual nonresonant mechanism, with a transfer of binding energy from the $dd\mu$ molecule to a conversion electron, is small, only 0.04 – $0.05 \mu\text{s}^{-1}$ at $T = 20$ K. This rate increases with the energy, reaching $\approx 0.5 \mu\text{s}^{-1}$ at $E = 1$ eV (Ref. 22).

The existence of a weakly bound level ($J = v = 1$) in the $dd\mu$ molecule, with an energy $\epsilon_{1,1} \approx 2$ eV, gives rise to a resonance mechanism^{2,10} for the production of $dd\mu$ molecules. This happens when the binding energy of the molecule, along with the kinetic energy of the $d\mu$ atom, is expended in exciting rotational-vibrational levels of the molecular complex $[(dd\mu), d, 2e]_{v,K_f}^*$:

$$\epsilon_{d\mu} + \epsilon_{1,1} = \Delta E_{v,K_f}, \quad (2)$$

where $v_f = 7$ and K_f are the vibrational and rotational quantum numbers of the complex, and $\epsilon_{d\mu}$ is the energy of the relative motion of the $d\mu$ atom and the D_2 molecule. Since the excitation energy $\Delta E_{v,K_f}$ takes on discrete values, this process can occur only at certain resonant energies $\epsilon_{d\mu}^r$. For thermalized $d\mu$ atoms, the rate of this process is

$$\Lambda = \int \sum_{i,f} W_{K_i} |M_{fi}|^2 \cdot 2\pi \delta(\epsilon_{d\mu} - \epsilon_{d\mu}^r) f(\epsilon_{d\mu}, T) d\epsilon_{d\mu}, \quad (3)$$

where W_{K_i} is the distribution with respect to the vibrational states K_i of the D_2 molecules, and f is a Maxwellian distribution. The calculated energies of $K_i \rightarrow K_f$ transitions are given in Ref. 15, where the hyperfine splitting of the $d\mu$ levels ($F = 3/2, 1/2$) and the $dd\mu$ levels (with spins $S = 3/2, 1/2$) is taken into account. It turns out that at low temperatures the $(F = 3/2) - (S = 1/2)$ transitions $K_i = 0 \rightarrow K_f = 1$ and $K_i = 1 \rightarrow K_f = 2$, with the resonant energies

$$\epsilon_{0-1}^r = 4,9 \text{ meV}, \quad \epsilon_{1-2}^r = 6,2 \text{ meV}, \quad (4)$$

dominate.

The incorporation of the width of the resonance $\epsilon_{d\mu}^r$ resulted in a further development of the theory for the resonance production of muonic molecules.^{11,12,17} In contrast with the Wessmann model, with fixed values of $\epsilon_{d\mu}^r$ [see expressions (2) and (3)], we should consider the width of the resonance, $\Phi = \Phi_0 - \Phi_{\text{coll}}$. Here $\Phi_0 = 0.001$ meV is the "vacuum" part, determined by the quantity $\bar{\lambda}_f \sim \lambda_f + \lambda_e$, where $\lambda_f = 0.43 \cdot 10^9 \text{ s}^{-1}$ is the rate of the $d + d$ reaction from the $J = v = 1$ state, and $\lambda_e \approx 0.03 \cdot 10^9 \text{ s}^{-1}$ is the rate of the deexcitation $(J, v = 1, 1) \rightarrow (J, v = 1, 0)$ (Refs. 23 and 24). The collisional width increases with the temperature:^{12,13}

$$\Phi_{\text{coll}} = 0,8 \phi T^{1/2} \ln^2(250/T) \text{ meV}. \quad (5)$$

According to Refs. 12 and 13, at small values of ϕ , with $\Phi_{\text{coll}} \ll \epsilon_{d\mu}^r$, the Wessmann model, (3). At $\phi \approx 1$ and $T = 70$ – 90 K, the collisional width becomes equal to the resonance energy in (4). In this case, the δ -function in (3) should be replaced by a Breit-Wigner expression. Specific calculations were carried out in Refs. 11 and 13, where it was shown that

the magnitude of the density effect in the rate $\lambda_{3/2}$ could reach 15–20%.

Competing with the nuclear reaction and the deexcitation of the complex is the inverse decay of the complex into $d\mu$ and D_2 (Refs. 25 and 10), at a rate $\Gamma = \Gamma_{1/2} + \Gamma_{3/2} \approx 1.5 \cdot 10^9$. Consequently, the rate at which $dd\mu$ molecules are produced, $\lambda_F = \Lambda_F \bar{\lambda}_F / (\Gamma + \bar{\lambda}_F)$ (determined from the fusion products), is smaller by a factor of several units than the rate at which the complex is produced. An important point is that changes may occur in the populations of the hyperfine levels of the $d\mu$ atom in the inverse decay.^{10,26} Such changes would lead to an effective increase (of about 30%) in λ_d , the rate of the ($F = 3/2$)-($F = 1/2$) transition.

The schematic diagram for the processes in Fig. 2 corresponds to a system of equations for the functions $N_{1/2}(t)$, $N_{3/2}(t)$ and $\bar{N}_n(t)$ (Refs. 5, 10, 18, and 27). If the lifetime of the complex is ignored ($t > 1/\lambda_f$), these equations become

$$\begin{aligned} dN_{3/2}/dt &= -(\lambda_0 + \lambda_d + \lambda_{3/2})N_{3/2} + \lambda_{3/2}N_{1/2} \\ &\quad + [^2/s(1-\omega)\lambda_{3/2} + \lambda_d']N_{3/2}, \\ dN_{1/2}/dt &= -(\lambda_0 + \lambda_d + \lambda_{1/2})N_{1/2} + \lambda_{1/2}N_{3/2} \\ &\quad + [^1/s(1-\omega)\lambda_{1/2} + \lambda_d]N_{1/2}, \\ d\bar{N}_n/dt &= (\lambda_{3/2}\beta_{3/2}N_{3/2} + \lambda_{1/2}\beta_{1/2}N_{1/2}), \end{aligned} \quad (6)$$

where $\lambda_0 = 0.455 \mu s^{-1}$ is the muon decay rate, $\omega = \beta\omega_d$, β is the partial probability for reaction (1b), $\omega_d = 0.12$ is the sticking coefficient for the attachment of the muon to helium in reaction (1a) (Ref. 19), $N_{3/2}$ and $N_{1/2}$ are the numbers of $d\mu$ atoms in the upper and lower hyperfine states, and N_n is the number of neutrons from all catalysis cycles caused by one muon. Analysis of Eqs. (6) leads to the conclusion that the temporal distribution ($d\bar{N}_n/dt$) is the sum of two exponential functions, a "fast" one and a "slow" one:

$$d\bar{N}_n/dt = F(t) = A_f \exp(-\lambda_f t) + A_s \exp(-\lambda_s t). \quad (7)$$

The approximate analytic solutions of system (6) (the error of the approximation is a few percent), i.e., the quantities A_f , λ_f , A_s , and λ_s , were derived as functions of the unknown parameters $\lambda_{3/4}$, $\lambda_{1/2}$, and λ_d in Ref. 10.

Experimentally, it is customary to analyze the temporal distribution N_n of the first neutrons which are detected. In this case, the efficiency ε_n with which these neutrons are detected must be taken into consideration.²⁸ In Refs. 28 and 29 we studied the kinetics of muon-catalyzed fusion by ignoring spin effects (there was one exponential in the temporal distribution). It turned out that in this case the solution for the first neutrons detected is the same as the solution for all neutrons ($\varepsilon_n \approx 0$), when the following substitution is made in the latter:

$$\omega = \beta\omega_d \rightarrow \beta(\omega_d + \varepsilon_n - \omega_d\varepsilon_n). \quad (8)$$

The kinetics of process (1) with spin effects and a finite detection efficiency was studied in Ref. 27. Exact solutions of system (6) were derived there for all neutrons, \bar{N}_n . The substitution in (8) was used to make the transition to solu-

tions for the first neutrons. Here are the approximate analytic solutions:

$$\begin{aligned} \lambda_f &\approx \lambda_0 + (\lambda_d + \lambda_d' + ^1/s\lambda_{3/2} + ^2/s\lambda_{1/2})\phi, \\ \lambda_s &\approx \lambda_0 + (\omega_d + \varepsilon_n - \omega_d\varepsilon_n)\lambda_{3/2}\beta\phi, \\ A_f &\approx 2(\lambda_{3/2} - \lambda_{1/2})A_M/3\lambda_{3/2}, \quad A_M = \lambda_{SS} = k\lambda_{3/2}\beta\phi. \end{aligned} \quad (9)$$

The quantity λ_{SS} is the rate of production of $dd\mu$ molecules, averaged over the spin states, for $t > \lambda_f^{-1}$ (this rate was measured in our previous studies^{7,20} and in some studies^{6,19} by a group from the Leningrad Institute of Nuclear Physics). The values of the coefficient k depend on the experimental conditions (on T and ε) and may differ from unity by 5–15%.

3. EXPERIMENTAL PROCEDURE; THE MEASUREMENTS

Figure 3 is a schematic diagram of the experimental apparatus. The basic parts are a cryogenic high-pressure (0.6-kbar) deuterium target³⁰ and a total-absorption scintillation neutron spectrometer.³¹ The target is made of a special steel (80% Ni + 16% Cr + 2% Al). Its inside diameter is 64 mm, and its inside height is 87 mm. The thickness of its side walls is 6 mm. Impurities with $Z > 1$ are removed by passing the deuterium through a palladium filter at 500 °C. This purification procedure results in a purity $\approx 10^{-7}$ by volume. The protium content in the target was less than 0.5%. The target was placed in a cryostat (not shown in Fig. 3), which made it possible to vary the target temperature over the range $T = 20$ –300 K and to hold a given temperature constant within ± 1 K.

The neutron spectrometer consisted of two identical detectors (ND), positioned symmetrically with respect to the target. The dimensions of the cell for the scintillator ($NE-213$) were a diameter of 31 cm and a height of 16.5 cm (each cell had a volume $V = 12$ liters). Neutrons and γ rays (or electrons) were separated on the basis of the shape of the scintillation pulse.³² Using a material equivalent to Teflon as a reflecting cover on the cell (on the one hand) and putting the photomultiplier in direct optical contact with the scintillator (on the other) made it possible to achieve good spectrometric properties for the ND detectors.³³ The overall

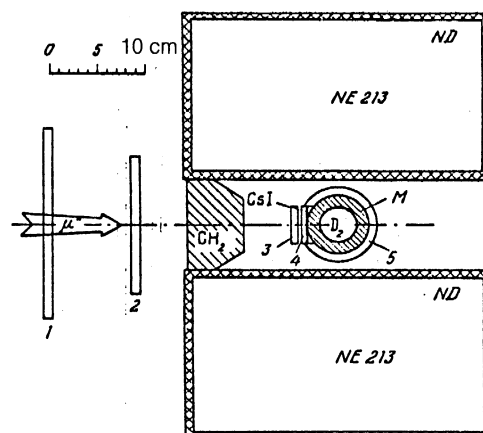


FIG. 3. Simplified diagram of the experimental apparatus. 1–5—Scintillation detectors; T—target; ND—neutron detectors.

efficiency of the detection by the two *ND* detectors for reaction (1) was about 30% (that in the experiments of Refs. 9 and 18 was only 2–3%).

Detectors 1–4 were used to detect the beam muons. Detector 5, which was a cylindrical scintillator (with a wall thickness of 7 mm) surrounding the target, was used to detect both muons and electrons from the decay of muons. For this purpose, the signal from this detector was branched into two channels. Special measures were taken to maintain good spectrometric properties for this detector. It thus became possible to reliably discriminate neutrons from reaction (1b) (with an energy release less than 0.7 MeV) by introducing a pulse-height threshold in the electron detection channel. At the same time, a high electron detection efficiency was retained (an energy evolution of at least 1.5 MeV).

An electronic trigger acted in such a way that “neutron” events were selected for subsequent analysis on a computer. The conditions which qualified events as neutron events were the presence of signals representing the detection of a neutron by one of the *ND* detectors (signal 5, *ND*) and the detection of that electron by detector 5 in a temporal gate 10 μ s wide coming after the signal (1–4, 5) representing the stopping of a muon in the target³⁴ (delayed *n-e* coincidences). A further condition was that there be no second signal for either the muon or the electron during the temporal gate. The temporal distributions of the electrons (the signals from detector 5) were recorded independently and were used to normalize the neutron events.

The lifetime of the fast component in the temporal distribution of the neutrons, (7), i.e., $\tau = 1/\lambda_f \approx 1/(\lambda_d \phi)$, was only 20–30 ns at $\phi \approx 1$. It was necessary to measure short times accurately with the neutron detectors and to reliably determine the zero for the time scale. Necessary changes (with respect to our previous studies^{7,8,20}) were accordingly made in the experiments. In order to reduce the “short-lived” neutron background (with $\tau = 200$ ns) from nuclear muon capture in the material of the target walls (an event was detected only in the case of a random signal from detector 5), and also to reduce the number of false triggers signalling an electron, we used a coincidence signal (5, *ND*). The events themselves were recorded only under the condition $t_e > 0.5 \mu$ s, where t_e is the electron detection time. A thorough study was made of the temporal parameters of the neutron detection system: the time resolution, the stability of the time zero, the calibration accuracy, and so forth.³⁵ For an

independent determination of the time zero, we measured the temporal distribution of the mesoroentgen γ rays throughout the experiment. These γ rays resulted from the stopping of muons in the target walls. The results of these measurements are evidence that the position of the time zero is stable to within 0.2 ns.

A total of eight main exposures with deuterium were carried out. The target temperature was varied from $T = 22$ K (liquid deuterium) to $T = 205$ K. The conditions during the experiments deuterium are listed in Table I. We also carried out exposures with helium, to determine the neutron background, and with an evacuated target, to determine the electron background. The number of electrons detected in each exposure was several million, while the number of neutrons from the process of interest was in the tens of thousands.

4. ANALYSIS OF EVENTS; RESULTS OF THE MEASUREMENTS

The analysis of the events which were recorded consisted of distinguishing neutrons from γ rays and electrons and constructing and analyzing pulse-height (energy) distributions and temporal distributions, separately for each particle species. We selected only those events for which the condition $t_e - t_n = 0.5\text{--}4.5 \mu$ s held, where t_n is the time at which the neutrons were detected.

Figure 4 shows representative temporal distributions of the neutrons for the two “extreme” temperatures, $T = 22$ and 205 K. We see that these distributions are a superposition of two exponential distributions, with very different arguments. The following results demonstrate that both components—the fast component and the slow one—are caused by events from reaction (1b).

1) The results of the measurements of the background carried out with a helium-filled target support this interpretation. The primary sources of the background are the random load on *ND* and the neutrons from nuclear muon capture in the target walls. The detection condition—the signal from detector 5 (in actuality, a 5, *ND* coincidence)—was satisfied in the first case by an electron from the decay of a muon which stopped in the target, while it was satisfied in the second case by a random load on detector 5. The use of *ND*, with a large geometric detection efficiency, and detector 5, with a low background load, kept the relative contribution of the background small, at most 5% (the worst case was that of the slow component at low temperatures).

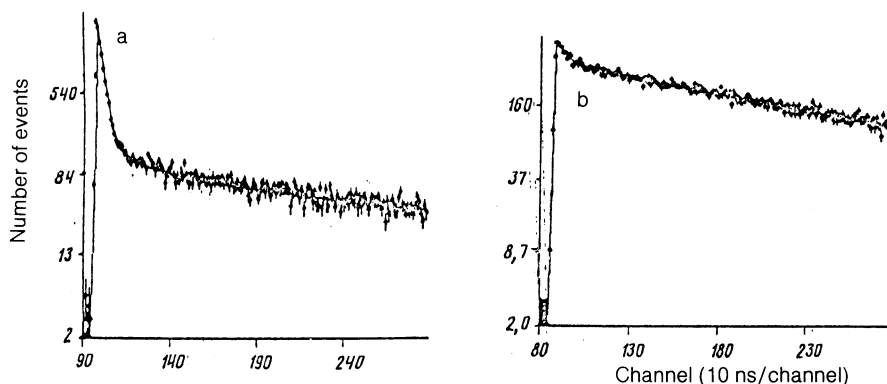


FIG. 4. Representative temporal distributions of the first neutrons detected. a—Exposure at $T = 22$ K; b—205 K. The points are experimental data; the lines show a fit of distribution (10) to the experimental points.

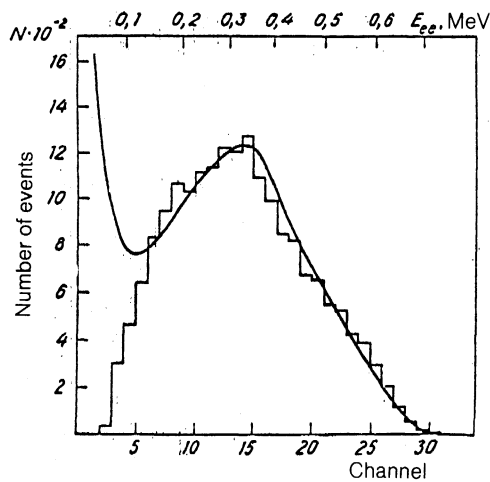


FIG. 5. Pulse-height distribution of the neutrons (or of the recoil protons) measured in one exposure with deuterium. The solid line is the result³⁶ of calculations by a program for finding the neutron detection efficiency.

2) The second piece of support comes from the nature of the pulse-height distribution of the neutrons. Specifically, the spectrum has the same shape for the events belonging to each component of the temporal distribution, and it has the same shape as would be expected on the basis of the calculations. Figure 5 shows a pulse-height distribution of the neutrons (recoil protons) measured by one of the ND 's in an exposure with deuterium. The solid line here shows results calculated³⁶ by a program for finding the detection efficiency ε_n by the Monte Carlo method. This program incorporated the interaction of neutrons with deuterium in the target, with the material of the target walls, and with the matter near the target. The loss in efficiency due to the pulse-height threshold was determined by means of an energy calibration of the analyzer scale with the help of standard γ sources and also through direct comparison of the measured distribution (for short times, at which there is essentially no background) with the calculated distribution. The threshold E^{thr} was set at a value which ensured reliable discrimination of the γ rays. The value of ε_n depends on the deuterium density in the target, because of the effect of n - d interactions. For the particular detection threshold selected, $E_e^{\text{thr}} = 140$ keV (the equivalent electron energy), the efficiency turned out to be $\varepsilon_n = 14.2 \pm 0.06\%$ (at a deuterium density $\phi = 0.885$) for each of the two ND 's.

The parameters of the process of interest were determined from an analysis of the temporal distributions of the neutrons. The distribution

$$dN_n/dt = CF(t) + B(t), \quad (10)$$

“convolved” with the time-resolution function of the detector, was fitted to these experimental distributions.³⁵ Here $F(t)$ is expression (7) for the temporal distribution of neutrons from reaction (1b), and $B(t)$ is the time evolution of the background. The parameter C is a normalization factor, which reflects the number of electrons detected from muon decay and also the neutron detection efficiency. In the course of the analysis, the parameters A_f , A_s , λ_f , and λ_s of expression (7) were varied to find the optimum values. We also varied the position of the time zero t_0 in the distribution and the time resolution of the detector.³⁵

In a first step, we analyzed exclusively the slow part ($t > 0.2 \mu\text{s}$) of the temporal distributions. This analysis made it possible to reliably determine the amplitude of the slow component, i.e., the equilibrium (steady-state) value λ_{ss} [see expression (9)]. In a second step, we fitted the complete distributions, optimizing λ_f , A_s , and the ratio A_f/A_s . To find the unknown values of $\lambda_{3/2}$, $\lambda_{1/2}$, and λ_d , we implemented an algorithm for the numerical solution²⁷ of Eqs. (6). The error of these calculations was 1–2%. In certain specific cases, we checked the results by the Monte Carlo method. For the partial probability $\beta_{3/2}$ we used the “resonance” value¹⁹ $\beta = 0.58$. To find $\beta_{1/2}$, we estimated the contribution from nonresonance production (assuming its rate to be independent of the temperature). We set $\beta = 0.50$.

We analyzed a possible effect of the finite lifetime of the $dd\mu$ molecule, which is ignored in Eqs. (6). We found that (1) our data are insensitive to this quantity within ± 1 ns and (2) the possible error in the determination of the amplitude A_f due to the neglect of the lifetime of the $dd\mu$ molecule is less than 1–2%.

Table I and Fig. 6 show the values found for $\lambda_{3/2}$ and $\lambda_{1/2}$ as a result of this analysis. The errors in these quantities include the statistical and systematic uncertainties. The most important of these components are the small uncertainties regarding the values of ε_n (4–5%) and ϕ . As Fig. 6 shows, in the case of the $\lambda_{1/2}(T)$ dependence our data agree well with the measurements of Refs. 9 and 18, carried out with low-density deuterium ($\phi = 0.02$ and 0.04), and also with the calculations of Refs. 10, 11, and 13. In terms of the

TABLE I. Results of measurements of the rate of production of $dd\mu$ molecules from various spin states of the $d\mu$ atoms (the rates are expressed in units of reciprocal microseconds).

T, K	ϕ	$\lambda_{1/2}$			$\lambda_{3/2}$		
		Value	Error		Value	Error	
			Statistical	Total		Statistical	Total
22±0.5	1.18±0.02	0.0421	0.0009	0.0023	2.69	0.08	0.15
48±1.5	0.88±0.04	0.0516	0.0012	0.0035	3.38	0.13	0.25
80±0.5	0.88±0.04	0.134	0.003	0.009	3.67	0.12	0.26
91±0.5	0.88±0.04	0.201	0.004	0.013	3.78	0.12	0.26
105±1.0	0.88±0.04	0.324	0.007	0.021	3.74	0.12	0.26
120±1.0	0.88±0.04	0.507	0.011	0.035	3.82	0.13	0.26
162±1.0	0.50±0.02	1.122	0.022	0.078	4.42	0.20	0.34
205±0.5	0.50±0.02	1.851	0.037	0.126	4.81	0.35	0.46

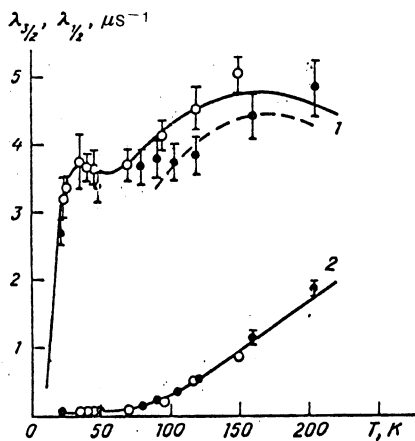


FIG. 6. Temperature dependence of (1) $\lambda_{3/2}$ and (2) $\lambda_{1/2}$ according to the present measurements and the experiments of Refs. 9 and 18. ●—Data of the present experiments; ○—data of the experiments of Refs. 9 and 18. Solid lines) Calculations of Ref. 11 on the basis of the Wessmann model; dashed line) calculations of Ref. 11 with allowance for the broadening of the resonance in the production of $dd\mu$ molecules.

$\lambda_{3/2}(T)$ dependence we find some discrepancy between our results and (first) the calculations of Ref. 11, carried out by the standard Wessmann model, and (second) the experimental data of Refs. 9 and 18. For the six points from the present experiments for the temperature interval $T = 80$ – 205 K, the deviation from the optimum $\lambda_{3/2}(T)$ dependence found in Ref. 18 by the calculation method of Refs. 10, 11, and 13 corresponds to a value $\chi^2 = 16$.

The discrepancy becomes more obvious when we express the experimental data as the ratio $\alpha = \lambda_{3/2}/\lambda_{1/2}$ and thereby essentially eliminate the systematic errors due to the uncertainties in the values of ϵ_n and ϕ . These errors are essentially the same for $\lambda_{3/2}$ and $\lambda_{1/2}$. In Fig. 7, we show the ratio $\alpha = \lambda_{3/2}/\lambda_{1/2}$ for our data and for the measurements of Ref. 9 and 18, after multiplication by the calculated values of $\lambda_{1/2}$ taken from Ref. 11. Since we do not know the experimental details of Refs. 9 and 18, it is likely that we have slightly overestimated the errors in the values of α for those experiments. We see from this figure that our points lie significantly below the optimum $\lambda_{3/2}(T)$ functional dependence found in Ref. 18.

At the same time, our values of $\lambda_{3/2}(T)$ agree fairly well with calculations based on the existing theory,^{11–13,17} which

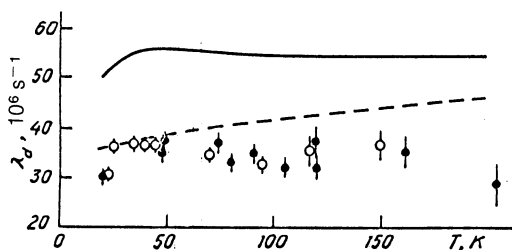


FIG. 7. Values of α , which is the ratio of $\lambda_{3/2}$ and $\lambda_{1/2}$, according to the measurements of Refs. 9 and 18 and also the measurements of the present study. These ratios have been multiplied by the theoretical¹¹ values of $\lambda_{1/2}$. ●—Data of the present experiments; ○—data of the measurements of Refs. 9 and 18; line—optimum $\lambda_{3/2}(T)$ dependence found in Ref. 18.

incorporates the broadening of the resonance in collisions between the complex $[(dd\mu), d, 2e]^*$ and D_2 molecules (the so-called collisional broadening of the resonance). The dashed line in Fig. 6 shows the results of corresponding calculations¹¹ for $\phi = 1.2$. The discontinuity at temperatures at which the “elastic” width is approximately equal to the resonance energy is evidence that there is room for improvement in calculations based on certain models. Nevertheless, the nature of the change in the rate $\lambda_{3/2}$ as the density is raised to $\phi \approx 1$ can be seen clearly, and there is agreement, at least qualitative, with experiment.

It is thus possible to reconcile the two sets of experimental data on $\lambda_{3/2}(T)$ —our own data, measured at a high deuterium density ($\phi \approx 1$) and the data obtained in Refs. 9 and 18 at a low density ($\phi \ll 1$)—on the basis of a theory which incorporates a dependence of $\lambda_{3/2}$ on the density as the result of collisional broadening of the resonance. It can thus be concluded that a density effect may be operating in the production of the muonic molecules $dd\mu$ from the upper spin state of the $d\mu$ atom. It would be important to carry out measurements of $\lambda_{3/2}(T)$ at $\phi \approx 1$ and ≈ 0.1 under the same experimental conditions in order to learn more about this question.

Figure 8 and Table II show values found for the rate λ_d of $(F = 3/2) \rightarrow (F = 1/2)$ transitions between hyperfine states of the $d\mu$ atoms according to this analysis of the experimental data. We recall that these are “effective” values, determined by the change in the spin of the $d\mu$ atoms not only in $d\mu + d$ collisions but also as a result of the inverse decay of the complex $[(dd\mu), d, 2e]$ (Refs. 26 and 10).

We see in Fig. 8 that our values of λ_d , obtained at $\phi \approx 1$, agree well with the experimental results of Refs. 9 and 18 for $\phi = 0.02$ and 0.04 , with the value $\bar{\lambda}_d = 37.3 \pm 1.5 \mu\text{s}^{-1}$, averaged over the temperature, which was found in Ref. 6 for $\phi = 0.1$. On the other hand, the experimental data on λ_d do not agree at all well with the calculations of Ref. 21 when we take account of the increase in the rate of $(F = 3/2) \rightarrow (F = 1/2)$ transitions due to the decay of the $[(dd\mu), d, 2e]$ complex.²⁶ This question requires further theoretical study.

We conclude with a look at measurements of the rate at which the $d\mu$ atoms are thermalized. The particular way in which $\lambda_{dd\mu} = \lambda_{3/2} + \lambda_{1/2}$ depends on the energy of the $d\mu$ atoms presents a unique opportunity for finding an estimate of this rate, by working from the delay t_{n0} in the beginning of

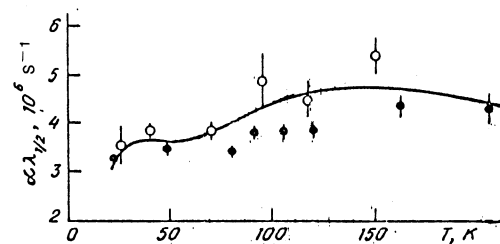


FIG. 8. Rate of the transition between hyperfine states of the $d\mu$ atom versus the deuterium temperature. ●—Data of the present study and results of Ref. 8; ○—measurements of Refs. 9 and 18; dashed line—calculations of Ref. 21 for the rate of the transition $(F = 3/2) \rightarrow (F = 1/2)$ in $d\mu + d$ collisions; solid line—the same, with allowance for the change in the populations of the hyperfine states of the $d\mu$ atom during the inverse decay of the complex $[(dd\mu), d, 2e]$ (Refs. 26 and 10).

TABLE II. Results of measurements of the rate of transition between hyperfine states of the $d\mu$ atom.

ϕ	1,18	0,88					0,5		
T, K	22	48	80	91	105	120	162	205	
$\lambda_d, \mu s^{-1}$	30,1	35,1	33,4	35,1	32,3	32,1	35,5	28,8	
Error	Statist.	0,5	0,7	0,7	0,8	1,0	1,0	2,4	4,0
	Total	0,7	1,7	1,7	1,8	1,9	1,9	2,9	4,3

the neutron temporal distribution with respect to the time at which the muon is stopped, $t_{\mu 0}$. To determine $t_{\mu 0}$ in the present study we measured the distribution of "instantaneous" (with 10^{-11} s) mesoroentgen γ rays which arise during atomic capture of muons in the material of the target walls. We found the value of t_{n0} by analyzing the neutron temporal distributions. A comparison of the measured difference $\Delta = t_{n0} - t_{\mu 0}$ with the calculated time of flight of the neutrons from the target to the detector leads to the conclusion that the time scale for the thermalization of the $d\mu$ atoms in deuterium under our conditions (with a density $\phi \approx 1$) is less than 2 ns. This result agrees with calculations²¹ of the cross section for the scattering $d\mu + d$. It would be interesting to see experiments with low-density deuterium which are more sensitive to the thermalization time.

We wish to thank L. I. Men'shikov, L. I. Ponomarev, and M. P. Faifman for useful discussions. We also thank B. M. Kulagin and M. M. Petrovskii for assistance in preparing the apparatus and in carrying out the measurements.

- ¹ V. P. Dzhelepov, P. F. Ermolov, V. I. Moskalev *et al.*, Zh. Eksp. Teor. Fiz. **50**, 1235 (1966) [Sov. Phys. JETP **23**, 820 (1966)].
² E. A. Vesman, Pis'ma Zh. Eksp. Teor. Fiz. **5**, 113 (1967) [JETP Lett. **5**, 91 (1967)].
³ S. I. Vinit'skii *et al.*, Zh. Eksp. Teor. Fiz. **74**, 849 (1978) [Sov. Phys. JETP **47**, 444 (1978)].
⁴ V. M. Bystritskii *et al.*, Zh. Eksp. Teor. Fiz. **76**, 460 (1979) [Sov. Phys. JETP **49**, 232 (1979)].
⁵ P. Kammel *et al.*, Phys. Lett. B **112**, 319 (1982); Phys. Rev. A **28**, 2611 (1983).
⁶ D. V. Balin *et al.*, Muon Catalyzed Fusion **2**, 241 (1988); **5/6**, 163 (1990/1991).
⁷ V. M. Bystritsky *et al.*, Muon Catalyzed Fusion **5/6**, 141 (1990/1991).
⁸ V. V. Filchenkov and L. Marczi's, Muon Catalyzed Fusion **5/6**, 499 (1990/1991).
⁹ W. Breunlich *et al.*, Muon Catalyzed Fusion **5/6**, 149 (1990/1991); J. Zmeskal *et al.*, Muon Catalyzed Fusion **1**, 109 (1987).
¹⁰ P. I. Men'shikov, P. I. Ponomarev, T. A. Strizh, and M. P. Faifman, Zh. Eksp. Teor. Fiz. **92**, 1173 (1987) [Sov. Phys. JETP **65**, 656 (1987)].
¹¹ M. P. Faifman, Muon Catalyzed Fusion **2**, 247 (1988).

- ¹² L. I. Menshikov, Muon Catalyzed Fusion **2**, 273 (1988); L. I. Men'shikov, Fiz. Elem. Chastits At. Yadra **19**, 1349 (1988) [Sov. J. Part. Nucl. **19**, 583 (1988)].
¹³ L. I. Menshikov, T. A. Strizh, and M. P. Faifman, Muon Catalyzed Fusion **4**, 1 (1989).
¹⁴ L. I. Ponomarev, Muon Catalyzed Fusion **3**, 629 (1988).
¹⁵ S. S. Gershtein, Yu. V. Petrov, and P. I. Ponomarev, Usp. Fiz. Nauk **160**, 3 (1990) [Sov. Phys. Usp. **33**, 1 (1990)].
¹⁶ D. Bakalov, Muon Catalyzed Fusion **3**, 321 (1988); G. Aissing, D. Bakalov, and H. Monkhorst, Phys. Rev. A **42**, 116 (1990).
¹⁷ Yu. V. Petrov, Phys. Lett. B **163**, 588 (1985).
¹⁸ J. Zmeskal *et al.*, Phys. Rev. A **42**, 1165 (1990); N. Nagele *et al.*, Nucl. Phys. A **493**, 397 (1989).
¹⁹ D. V. Balin *et al.*, Pis'ma Zh. Eksp. Teor. Fiz. **40**, 318 (1984) [JETP Lett. **40**, 1112 (1984)].
²⁰ V. M. Bystritsky *et al.*, in *Muon Catalyzed Fusion (Proceedings of the Conference on Muon Catalyzed Fusion, Sanibel Island, 1988)* (ed. S. E. Jones, J. Rafelsky, and H. J. Monkhorst), AIP, New York, 1989 (AIP Conf. Proc., No. 81, p. 17).
²¹ A. Adamchak and V. S. Melezhik, Muon Catalyzed Fusion **4**, 303 (1989).
²² M. P. Faifman, Muon Catalyzed Fusion **4**, 341 (1989).
²³ L. N. Bogdanova, Muon Catalyzed Fusion **3**, 359 (1988).
²⁴ D. Bakalov *et al.*, Zh. Eksp. Teor. Fiz. **94**(10), 61 (1988) [Sov. Phys. JETP **67**(10), 1990 (1988)].
²⁵ A. M. Lane, Phys. Lett. A **98**, 337 (1983).
²⁶ M. Leon, Phys. Rev. A **33**, 4434 (1986).
²⁷ V. V. Filchenkov, Communications JINR E1-89-57, Dubna, 1989.
²⁸ V. G. Zinov, L. N. Somov, and V. V. Fil'chenkov, Preprint P15-82-478, Joint Institute for Nuclear Research, Dubna, 1982; At. Energ. **58**, 190 (1985).
²⁹ V. V. Filchenkov, L. N. Somov, and V. G. Zinov, Nucl. Instrum. Methods A **228**, 174 (1984).
³⁰ V. M. Bystritskii *et al.*, Prib. Tekh. Eksp. No. 1, 50 (1989).
³¹ V. P. Dzhelepov *et al.*, Nucl. Instrum. Methods A **269**, 634 (1988).
³² V. G. Zinov, E. Donski, and A. I. Rudenko, Prib. Tekh. Eksp. No. 1, 91 (1991).
³³ V. V. Filchenkov, A. D. Konin, and A. I. Rudenko, Nucl. Instrum. Methods A **294**, 504 (1990).
³⁴ A. I. Gilev *et al.*, Report P13-90-452, Joint Institute for Nuclear Research, Dubna, 1990.
³⁵ V. G. Zinov *et al.*, Preprint P13-91-182, Joint Institute for Nuclear Research, Dubna, 1991.
³⁶ V. V. Filchenkov and L. Marczi's, Communications JINR E13-88-566, Dubna, 1988.

Translated by D. Parsons